Geomechanics and Engineering, *Vol. 36, No. 4 (2024) 407-416*
https://doi.org/10.12989/gae.2024.36.4.407

Dynamic bending of sandwich nanocomposite rock tunnels by concrete beams

Liji Long[1] and D.L. Dung*[2]

[1]*Southwest Research Institute for Hydraulic and Water Transport Engineering, Chongqing Jiaotong University, Chongqing 400074, China*
[2]*Department of Mechanical Engineering, University of Hong Kong, Hong Kong*

(*Received February 14, 2023, Revised January 10, 2024, Accepted February 5, 2024*)

Abstract. Dynamic response of a rock tunnels by laminated porous concrete beam reinforced by nanoparticles subjected to harmonic transverse dynamic load is investigated considering structural damping. The effective nanocomposite properties are evaluated on the basis of Mori-Tanaka model. The concrete beam is modeled by the exponential shear deformation theory (ESDT). Utilizing nonlinear strains-deflection, energy relations and Hamilton's principal, the governing final equations of the concrete laminated beam are calculated. Utilizing differential quadrature method (DQM) as well as Newmark method, the dynamic displacement of the concrete laminated beam is discussed. The influences of porosity parameter, nanoparticles volume percent, agglomeration of nanoparticles, boundary condition, geometrical parameters of the concrete beam and harmonic transverse dynamic load are studied on the dynamic displacement of the laminated structure. Results indicated that enhancing the nanoparticles volume percent leads to decrease in the dynamic displacement about 63%. In addition, with considering porosity of the concrete, the dynamic displacement enhances about 2.8 time.

Keywords: DQM; dynamic response; laminated concrete porous beam; nanoparticles; newmark method; rock tunnels

1. Introduction

Various porous materials such as concrete or metal foams have distinctive attraction for widespread applications in mechanic, aerospace and civil engineering (Sang *et al.* 2015, Harith 2018, Azree and Wang 2012, Zhang *et al.* 2021). Furthermore, considerate the dynamic bending of porous composite concrete slabs and beams is vital for civil engineering applications. With the excellent mechanical behavior and high capability of energy-absorbing, concrete foams are one of the prominent candidates for the concrete structures subjected to dynamic loads (Bai *et al.* 2019, Pietras and Sadowski 2019, Craveiro *et al.* 2020, Sridhar and Prasad 2019, Sahoo *et al*. 2021, Chan *et al.* 2020, Alipour and Shariyat 2019). Porous materials containing nanoparticles makes novel nanocomposite concrete structures with excellent mechanical material properties.

In the field of experimental and numerical investigations of reinforced concrete structures, Gemi *et al.* (2019) investigated the shear capacity and damage analysis of thinned end prefabricated concrete purlins strengthened by CFRP composite experimentally. Various damage modes of the structure such as delamination, cover separation, debonding, fiber bundles breakage, air voids, matrix cracks, fiber bundles debonding, fiber breakage and buckling were observed thoroughly. Aksoylu *et al.* (2020a) considered the damages occurred at dapped-end region of prefabricated purlins due to snow load accumulated at the roof. Aksoylu *et al*. (2020b) offered an experimental analysis for reinforced concrete shear deficient beams with circular web openings strengthened by CFRP composite. They showed a significant decrease in load carrying capacities with the hole diameters increase. Also, they concluded that the load carrying capacity and ductility can be significantly improved owing to different CFRP configurations. Özkılıç *et al*. (2021a) presented a numerical evaluation for the effects of shear span, stirrup spacing and angle of stirrup on reinforced concrete beam behavior. They stated that as the shear span/effective depth ratio increases, the behavior of a shear deficient beam tends to typical bending behavior. Özkılıç *et al.* (2021b) presented an experimental and numerical investigations of steel fiber reinforced concrete dapped-end purlins. They specified that the use of steel fiber reinforced concrete (SFRC) increases the energy dissipation and shear capacities approximately 2.58 and 1.53 times, respectively. Özkılıç *et al*. (2021c) presented a series of numerical modelling with the finite element program ABAQUS in order to investigate the behavior of prefabricated concrete purlins (PCPs) through parametric study. In addition to the mechanical properties of the PCPs, the strengthening of the PCPs with the help of carbon fiber reinforced polymers (CFRP) was considered as a parameter in the models. Aksoylu *et al*. (2021) investigated the load carrying capacities of precast purlin beams with thin ends experimentally and numerically.

A few researches have been done on the mathematical modeling and mechanical behavior in various concrete elements. Vibration response of concrete foundations resting on soil medium strengthened by nano fiber reinforced polymer (NFRP) layer was studied by Zamani

*Corresponding author, Professor
E-mail: dldung.vnu@gmail.com

ISSN: 2005-307X (Print), 2092-6219 (Online)

and Rabani Bidgoli (2017) on the basis of ESST. They showed that enhancing the CNT volume fraction, the frequency of the structure rises. Zamanian *et al.* (2017) considered the agglomeration influences on the buckling analysis of concrete embedded columns containing SiO_2 nanoparticles. They revealed that with enhancing the SiO_2 nanoparticles volume percent in inclusion, the buckling load growths. Bakhshande Amnieh *et al.* (2018) considered the influences of various parameters of volume fraction and agglomeration of SiO_2 nanoparticles on the maximum velocity for the concrete non-homogenous block located on soil medium under the blast load theoretically and experimentally. Alijani and Rabani Bidgoli (2018) analyzed the vibration of concrete foundations reinforced by agglomerated SiO_2 nanoparticles on the basis of shear higher order theory of plates. They derived the coupled motion equations of structure using the Hamilton's principle and based on an analytical method, the frequency of system was obtained. Heidarzadeh *et al.* (2018) measured the thermal and mechanical stresses of the concrete tubes retrofitted by agglomerated AL_2O_3 nanoparticles. Seismic response of concrete plates retrofitted by AL_2O_3 nanoparticles on the basis of ESST was done by Amoli *et al.* (2018). Mathematical modeling for the vibration response of smart nanopaerticles-reinforced concrete foundations was prepared by Kargar and Bidgoli (2018). Jassas *et al.* (2019) investigated the forced vibration analysis in agglomerated SiO_2 nanoparticles-retrofitted concrete slabs utilizing numerical solution. Their Outcomes indicated that with increasing the SiO_2 nanoparticles volume fraction up to 0.37, the linear frequency increases and the dynamic maximum displacement decreases. In another research, Azmi *et al.* (2019) considered the dynamic blast behavior of concrete beam containing SiO_2 nanoparticles. A novel two variable shear deformation beam theories were developed and applied by Bedia *et al.* (2019) to investigate the combined effects of nonlocal stress and strain gradient on the bending and buckling behaviors of nanobeams by using the nonlocal strain gradient theory. Mahjoobi and Rabani Bidgoli (2019) calculated the vibration of SiO_2 nanoparticles-armed concrete foundations using numerical solution. Seismic response of pad concrete foundation strengthened by smart layer containing nanoparticles on the basis of higher order theory of plate was studied by Taherifar *et al.* (2020). Madenci *et al.* (2020a) presented a multiscale analysis of the deflection and stress behavior of pultruded GFRP composite beam. Madenci *et al.* (2020b) considered the buckling and free vibration of pultruded GFRP laminated composites by experimental, numerical and analytical methods. Madenci *et al.* (2020c) employed the experimental and theoretical methods for the flexure performance of pultruded GFRP composite beams with damage analyses. An efficient integral higher-order shear and normal deformation theory (IHSNDT) was developed by Draiche *et al.* (2021) based on a unified and enriched kinematic model to investigate the static bending phenomenon of functionally graded (FG) sandwich curved beams under uniform mechanical loads.

The thermal influences on dynamic properties of functionally graded (FG) nanobeams under various types of thermal environments were examined by Bendaida *et al.* (2022). An accurate kinematic model has been developed by Mouaici *et al.* (2022) to study the mechanical response of functionally graded (FG) sandwich beams, mainly covering the bending, buckling and free vibration problems. Mesbah *et al.* (2023) addressed the finite element modeling of functionally graded porous (FGP) beams for free vibration and buckling behaviour cases. Tounsi *et al.* (2023) investigated the free vibration of functionally graded material (FGM) sandwich plates supported by different boundary conditions and influenced by a three-parameter viscoelastic foundation and hygro-thermal changes.

In addition, dynamic bending of porous structure is one of the prominent problems in engineering fields which is extraordinary developed by researchers in beams, plates and shells structures. Although porosity can make thoughtful engineering problems but it can modify the mechanical analysis of structures with changing the porosity distributions. Hence, dynamic analysis of porous structure is essential. Viet and zaki (2021) derived a bending static theory for cantilever composite poroelastic beams including porous functionally graded (FG) shape memory alloy. Fouaidi *et al.* (2020) estimated the nonlinear bending analysis of Porous FG beams utilizing novel numerical method combined by meshless solution. In another research, Fouaidi *et al.* (2021) investigated the bending linear response of thin and straight composite FG beams armed by graphene oxide nanopowder and subjected to mechanical static loads on the basis of mesh free method. Anirudh *et al.* (2020) carried out the nonlinear dynamic bending of curved porous beams armed by nanocomposite beam using finite element solution method. Polit *et al.* (2019) scrutinized the elastic stability and static bending of thick FG nanocomposite curved porous beams. Penna *et al.* (2021) studied the bending analysis of FG porous nanobeams subjected to thermo-hygro-mechanical loads. Madenci and Ozkili (2021) explored the influence of porosity on free vibration analysis of functionally graded (FG) beams with different boundary conditions using different efficient analytical and numerical approaches. They estimated the material properties of open-cell FG porous beams using a modified power-law with two different types of porosity distributions through the thickness direction of the FG beam namely even and non-even distributions. Furthermore, the Artificial Neural Networks (ANNs) technique was used to predict the effects of porosity coefficient, porosity distributions, slenderness ratio and boundary conditions on natural frequency variations of porous FG beam.

As it is seen from the above discussions, the studies related to dynamic deflection of laminated porous beams are very limited. Therefore, it is crucial to determine the behavior of this material against dynamic loads considering the nanoparticles, porosity and lamina number. Hence, this paper describes the creative of a mathematical model to characterize the relationship between dynamic bending and porosity for beams made of porous concrete material reinforced with nanoparticles considering structural damping. The objectives from the outset for this paper are develop a mathematical framework for the dynamic

bending analysis of sandwich nanocomposite concrete beams, implement the ESST to capture accurate and realistic deformation behavior, apply DQM as a numerical technique for solving the dynamic bending equations, conduct a parametric study to explore the influence of key parameters. The Mori-Tanaka model is used for calculating the equivalent characteristics of structure. The laminated porous concrete beam is mathematically modeled with ESST and solved by DQM for obtaining the dynamic deflection of structure. The influences of porosity parameter, agglomeration and volume fraction of nanoparticles, boundary conditions, harmonic transverse dynamic load and geometrical parameters of beam are presented on the dynamic deflection of laminated porous concrete beam.

2. Mathematical modeling

Fig. 1 shows a laminated concrete porous beam reinforced by nanoparticles subjected to harmonic transverse dynamic load.

Using ESDT, the displacements in three directions are (Reddy 2002)

$$u_1(x,z,t)=u(x,t)-z\frac{\partial w(x,t)}{\partial x}+f\psi(x,t)\,, \tag{1}$$

$$u_2(x,z,t)=0\,, \tag{2}$$

$$u_3(x,z,t)=w(x,t)\,, \tag{3}$$

in which u_1, u_2 and u_3 are the mid plane deflections in the axial, transverse and thickness directions, respectively; ψ is the cross section rotation; $f=e^{-\frac{\pi z}{h}}$ Using Eqs. (1) to (3), the nonlinear strain equations on the basis of Von - Karman theory are

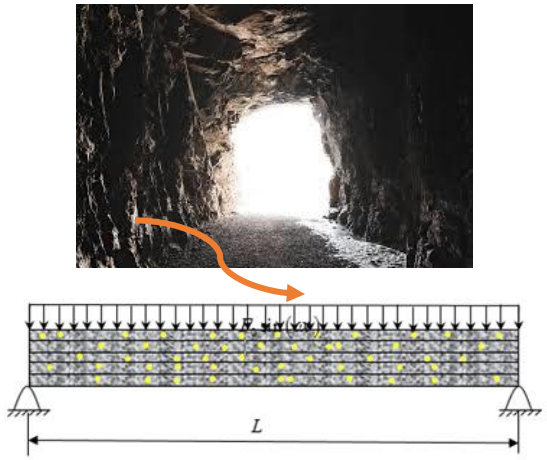

Fig. 1 A laminated porous concrete beam reinforced by nanoparticles under the harmonic transverse dynamic load

$$\varepsilon_{xx}=\frac{\partial u}{\partial x}-z\frac{\partial^2 w}{\partial x^2}+\frac{1}{2}\left(\frac{\partial w}{\partial x}\right)^2+f\frac{\partial \psi}{\partial x}, \tag{4}$$

$$\varepsilon_{xz}=f'\psi. \tag{5}$$

3. Mori-Tanaka model

Here, for obtaining the effective material properties of the concrete beam containing nanoparticles, the Mori-Tanaka model is used (Jafarian Arani and Kolahchi 2016). With assuming the Young's modulus E_m and the Poisson's ratio υ_m for the concrete beam, we have

$$\begin{Bmatrix}\sigma_{11}\\ \sigma_{22}\\ \sigma_{33}\\ \sigma_{23}\\ \sigma_{13}\\ \sigma_{12}\end{Bmatrix}=\begin{bmatrix}k+m & l & k-m & 0 & 0 & 0\\ l & n & l & 0 & 0 & 0\\ k-m & l & k+m & 0 & 0 & 0\\ 0 & 0 & 0 & p & 0 & 0\\ 0 & 0 & 0 & 0 & m & 0\\ 0 & 0 & 0 & 0 & 0 & p\end{bmatrix}\begin{Bmatrix}\varepsilon_{11}\\ \varepsilon_{22}\\ \varepsilon_{33}\\ \gamma_{23}\\ \gamma_{13}\\ \gamma_{12}\end{Bmatrix} \tag{6}$$

in which k, m, n, l, p are stiffness parameters which are defined as (Jafarian Arani and Kolahchi 2016)

$$\begin{aligned}
k&=\frac{E_m\{E_m c_m+2k_r(1+\nu_m)[1+c_r(1-2\nu_m)]\}}{2(1+\nu_m)[E_m(1+c_r-2\nu_m)+2c_m k_r(1-\nu_m-2\nu_m^2)]}\\
l&=\frac{E_m\{c_m\nu_m[E_m+2k_r(1+\nu_m)]+2c_r l_r(1-\nu_m^2)]\}}{(1+\nu_m)[E_m(1+c_r-2\nu_m)+2c_m k_r(1-\nu_m-2\nu_m^2)]}\\
n&=\frac{E_m^2 c_m(1+c_r-c_m\nu_m)+2c_m c_r(k_r n_r-l_r^2)(1+\nu_m)^2(1-2\nu_m)}{(1+\nu_m)[E_m(1+c_r-2\nu_m)+2c_m k_r(1-\nu_m-2\nu_m^2)]}\\
&\quad+\frac{E_m[2c_m^2 k_r(1-\nu_m)+c_r n_r(1+c_r-2\nu_m)-4c_m l_r\nu_m]}{E_m(1+c_r-2\nu_m)+2c_m k_r(1-\nu_m-2\nu_m^2)}\\
p&=\frac{E_m[E_m c_m+2p_r(1+\nu_m)(1+c_r)]}{2(1+\nu_m)[E_m(1+c_r)+2c_m p_r(1+\nu_m)]}\\
m&=\frac{E_m[E_m c_m+2m_r(1+\nu_m)(3+c_r-4\nu_m)]}{2(1+\nu_m)\{E_m[c_m+4c_r(1-\nu_m)]+2c_m m_r(3-\nu_m-4\nu_m^2)\}}
\end{aligned} \tag{7}$$

in which C_m and C_r are the matrix and the nanoparticles volume fractions respectively; k_r, l_r, n_r, p_r, m_r are the elastic Hills modulus. With assuming the agglomeration of nanoparticles, the volume fraction of nanoparticles can be divided to two fractions of in ''inclusions'' ($V_r^{inclusion}$) and out of ''inclusions'' (V_r^m) as

$$V_r=V_r^{inclusion}+V_r^m \tag{8}$$

For agglomeration of nanoparticles, we have two parameters of ξ and ζ as

$$\xi=\frac{V_{inclusion}}{V}, \tag{9}$$

$$\zeta=\frac{V_r^{inclusion}}{V_r}. \tag{10}$$

In addition, the average nanoparticle volume percent C_r is

$$C_r = \frac{V_r}{V}. \tag{11}$$

The effective shear (G) and bulk modulus (K) are (Jafarian Arani and Kolahchi 2016)

$$K = K_{out}\left[1+\frac{\xi\left(\frac{K_{in}}{K_{out}}-1\right)}{1+\alpha(1-\xi)\left(\frac{K_{in}}{K_{out}}-1\right)}\right], \tag{12}$$

$$G = G_{out}\left[1+\frac{\xi\left(\frac{G_{in}}{G_{out}}-1\right)}{1+\beta(1-\xi)\left(\frac{G_{in}}{G_{out}}-1\right)}\right], \tag{13}$$

in which

$$K_{in} = K_m + \frac{\left(\delta_r - 3K_m\chi_r\right)C_r\zeta}{3\left(\xi - C_r\zeta + C_r\zeta\chi_r\right)}, \tag{14}$$

$$K_{out} = K_m + \frac{C_r\left(\delta_r - 3K_m\chi_r\right)(1-\zeta)}{3\left[1-\xi-C_r(1-\zeta)+C_r\chi_r(1-\zeta)\right]}, \tag{15}$$

$$G_{in} = G_m + \frac{\left(\eta_r - 3G_m\beta_r\right)C_r\zeta}{2\left(\xi - C_r\zeta + C_r\zeta\beta_r\right)}, \tag{16}$$

$$G_{out} = G_m + \frac{C_r\left(\eta_r - 3G_m\beta_r\right)(1-\zeta)}{2\left[1-\xi-C_r(1-\zeta)+C_r\beta_r(1-\zeta)\right]}, \tag{17}$$

in which $\chi_r, \beta_r, \delta_r, \eta_r$ are

$$\chi_r = \frac{3\left(K_m+G_m\right)+k_r-l_r}{3\left(k_r+G_m\right)}, \tag{18}$$

$$\beta_r = \frac{1}{5}\left\{\begin{array}{l}\frac{4G_m+2k_r+l_r}{3\left(k_r+G_m\right)}+\frac{4G_m}{\left(p_r+G_m\right)}+\\ \frac{2\left[G_m\left(3K_m+G_m\right)+G_m\left(3K_m+7G_m\right)\right]}{G_m\left(3K_m+G_m\right)+m_r\left(3K_m+7G_m\right)}\end{array}\right\}, \tag{19}$$

$$\delta_r = \frac{1}{3}\left[n_r+2l_r+\frac{\left(2k_r-l_r\right)\left(3K_m+2G_m-l_r\right)}{k_r+G_m}\right], \tag{20}$$

$$\eta_r = \frac{1}{5}\left[\begin{array}{l}\frac{2}{3}\left(n_r-l_r\right)+\frac{4G_m p_r}{\left(p_r+G_m\right)}+\\ \frac{8G_m m_r\left(3K_m+4G_m\right)}{3K_m\left(m_r+G_m\right)+G_m\left(7m_r+G_m\right)}+\\ \frac{2\left(k_r-l_r\right)\left(2G_m+l_r\right)}{3\left(k_r+G_m\right)}\end{array}\right]. \tag{21}$$

in which, K_m and G_m are

$$K_m = \frac{E_m}{3(1-2\upsilon_m)}, \tag{22}$$

$$G_m = \frac{E_m}{2(1+\upsilon_m)}. \tag{23}$$

In addition, β, α are

$$\alpha = \frac{(1+\upsilon_{out})}{3(1-\upsilon_{out})}, \tag{24}$$

$$\beta = \frac{2(4-5\upsilon_{out})}{15(1-\upsilon_{out})}, \tag{25}$$

$$\upsilon_{out} = \frac{3K_{out}-2G_{out}}{6K_{out}+2G_{out}}. \tag{26}$$

In final, the effective poison's ratio (υ) and elastic modulus(E) may be given as (Jafarian Arani and Kolahchi 2016)

$$E = \frac{9KG}{3K+G}, \tag{27}$$

$$\upsilon = \frac{3K-2G}{6K+2G}. \tag{28}$$

The laminated concrete beam is porous. Hence we have (Keshtegar *et al.* 2020a)

$$E(z) = E_c\left[1-e_0\psi(z)\right] \tag{29}$$

$$\rho(z) = \rho_c\left[1-e_m\psi(z)\right] \tag{30}$$

in which ρ_c and E_c present the maximum parameters of $\rho(z)$ and $E(z)$, i.e., the material characteristic of a pure composite beam without pores, e_m=(1- ρ_2/ρ_1) and e_0=(1- E_2/E_1) are mass density coefficient and porosity coefficient. In addition, e_m, e_0 and e_p are from zero to one which presents the porosity of the beam. For various porosity distributions, $\psi(z)$ may be given as

$$\psi(z) = \left\{\begin{array}{ll}\cos\left(\frac{\pi z}{h}\right) & \textit{symmetric}\\ \cos\left(\frac{\pi z}{2h}+\frac{\pi}{4}\right) & \textit{asymmetric}\end{array}\right. \tag{31}$$

Where β = z/h, ρ, G and E are density, shear modulus and Young's modulus, respectively which can be calculated by Mori and Tanaka theory. In addition, the porosity parameter e_0 and the porosity parameter for density e_m can be related with $e_m = 1-\sqrt{1-e_0}$ (Keshtegar *et al*. 2020a).

4. Governing final equations

In this section, energy method is utilized. Based on this method, the strain energy may be given as (Reddy 2002)

$$U = \frac{1}{2}\int_V \left(\sigma_{xx}\varepsilon_{xx} + \sigma_{xz}\varepsilon_{xz}\right) dV\,, \tag{32}$$

Substituting Eqs. (4) and (5) in Eq. (32), strain energy is

$$U = \frac{1}{2}\int_V \begin{pmatrix} \sigma_{xx}\left(\frac{\partial u}{\partial x} - z\frac{\partial^2 w}{\partial x^2} + \frac{1}{2}\left(\frac{\partial w}{\partial x}\right)^2 + f\frac{\partial \psi}{\partial x}\right) + \\ \sigma_{xz}\left(\cos\left(\frac{\pi z}{h}\right)\psi\right) \end{pmatrix} dV\,, \tag{33}$$

The definition of in plane moments and forces are

$$\left(N_x, M_x, P_x\right) = \sum_{k=1}^{N}\int_{z^{(k-1)}}^{z^{(k)}} \sigma_{xx}^{(k)}\left(1, z, f\right) dz\,, \quad (i, j = 1,2,6) \tag{34}$$

$$Q_x = \sum_{k=1}^{N}\int_{z^{(k-1)}}^{z^{(k)}} \sigma_{xz}^{(k)} \cos\left(\frac{\pi z}{h}\right) dz\,, \quad (i, j = 1,2,6) \tag{35}$$

Using Eqs. (34) and (35), the strain energy may be simplified as

$$U = \int_x \begin{pmatrix} N_x\frac{\partial u}{\partial x} + \frac{N_x}{2}\left(\frac{\partial w}{\partial x}\right)^2 - \\ M_x\frac{\partial^2 w}{\partial x^2} + P_x\frac{\partial \psi}{\partial x} + Q_x\psi \end{pmatrix} dx \tag{36}$$

The kinetic energy of the laminated concrete porous beam is

$$\begin{aligned} K = 0.5\int \Bigg(& I_0\left(\left(\frac{\partial u}{\partial t}\right)^2 + \left(\frac{\partial w}{\partial t}\right)^2\right) + \\ & 2I_1\frac{\partial u}{\partial t}\frac{\partial w}{\partial t \partial x} + I_2\left(\frac{\partial w}{\partial t \partial x}\right)^2 + \\ & I_3\left(\frac{\partial \psi}{\partial t}\right)^2 + 2I_4\frac{\partial w}{\partial t \partial x}\frac{\partial \psi}{\partial t} + 2I_5\frac{\partial u}{\partial t}\frac{\partial \psi}{\partial t}\Bigg) dA. \end{aligned} \tag{37}$$

where the moment of inertias are

$$\left(I_0, I_1, I_2, I_3, I_4, I_5\right) = \sum_{k=1}^{N}\int_{z^{(k-1)}}^{z^{(k)}} \rho\left(1, z, z^2, f, f^2, zf\right) dz\,, \quad (i, j = 1,2,6) \tag{38}$$

The external work due to the harmonic transverse dynamic load is (Jassas *et al*. 2019)

$$W_b = \int \left(F_0 \sin\left(\omega t\right)\right) w dA, \tag{39}$$

Hamilton's principle is expressed as (Reddy 2002)

$$\int_0^t \left(\delta U - \delta K - \delta W_b\right) dt = 0, \tag{40}$$

Substituting Eqs. (36), (37) and (39) into Eq. (40) we have the below final equations:

$$\delta u : \frac{\partial N_x}{\partial x} = I_0\frac{\partial^2 u}{\partial t^2} - \mathrm{I}_1\frac{\partial^3 w}{\partial t^2 \partial x} + \mathrm{I}_5\frac{\partial^2 \psi}{\partial t^2}, \tag{41}$$

$$\delta w : \frac{\partial^2 M_x}{\partial x^2} + F_0 \sin\left(\omega t\right) = I_0\frac{\partial^2 w}{\partial t^2} + \mathrm{I}_1\frac{\partial^3 u}{\partial t^2 \partial x} - \mathrm{I}_2\frac{\partial^4 w}{\partial t^2 \partial x^2} + \mathrm{I}_5\frac{\partial^3 \psi}{\partial t^2 \partial x}, \tag{42}$$

$$\delta \psi : \frac{\partial P_x}{\partial x} - Q_x = I_3\frac{\partial^2 \psi}{\partial t^2} - I_4\frac{\partial^3 w}{\partial t^2 \partial x} + I_5\frac{\partial^2 u}{\partial t^2}, \tag{43}$$

5. DQM

On the basis of DQM, the differential equations may be changed to algebraic ones using (Hajmohammad *et al.* 2017, Keshtegar *et al.* 2020b, Al-Furjan *et al*. 2021, Motezaker *et al.* 2021, Shagholani Loor *et al.* 2020).

$$\frac{df}{dx} \overset{x=x_i}{\longrightarrow} = \sum_{j=1}^{N} C_{ij} f_j\,, \tag{44}$$

In which N is the grid points number of and C_{ij} is weighting coefficients which can be given as

$$X_i = \frac{L}{2}\left[1 - \cos\left(\frac{i-1}{N-1}\right)\pi\right] \quad i = 1, \ldots, N. \tag{45}$$

$$C_{ij}^{(1)} = \frac{L_1(x_i)}{(x_i - x_j)L_1(x_j)} \quad for \quad i \neq j, \quad i, j = 1, 2, \ldots, N\,, \tag{46}$$

$$C_{ii}^{(1)} = -\sum_{j=1, j\neq i} C_{ij}^{1} \quad for \quad i = j, \ i = 1, 2, \ldots, N\,, \tag{47}$$

where

$$L(x_i) = \prod_{\substack{j=1 \\ j\neq i}}^{N_x} (x_i - x_j). \tag{48}$$

In addition, the higher derivative weighting coefficients is

$$C_{ij}^{(n)} = n\left(C_{ii}^{(n-1)}C_{ij}^{(1)} - \frac{C_{ij}^{(n-1)}}{(x_i - x_j)}\right) \qquad i \neq j. \tag{49}$$

Boundary conditions for the laminated concrete beam are:

- **Clamped- Clamped (CC)**

$$\begin{aligned} w &= u = \varphi = \psi = 0, && @ \quad x = 0 \\ w &= u = \varphi = \psi = 0. && @ \quad x = L \end{aligned} \tag{50}$$

- **Clamped- Simple (CS)**

$$\begin{aligned} w &= u = \phi = \psi = 0, && @ \quad x = 0 \\ w &= u = \phi = \frac{\partial \psi}{\partial x} = 0. && @ \quad x = L \end{aligned} \tag{51}$$

- **Simple- Simple (SS)**

$$w = u = \phi = \frac{\partial \psi}{\partial x} = 0, \qquad @ \quad x = 0$$
$$w = u = \phi = \frac{\partial \psi}{\partial x} = 0. \qquad @ \quad x = L \tag{52}$$

In final, the matrix form of governing equations is

$$\left(\left[\underbrace{K_L + K_{NL}}_{K} \right] \begin{Bmatrix} \{d_b\} \\ \{d_d\} \end{Bmatrix} + [M] \begin{Bmatrix} \{\ddot{d}_b\} \\ \{\ddot{d}_d\} \end{Bmatrix} \right) = \begin{Bmatrix} \{0\} \\ F \end{Bmatrix}, \tag{53}$$

In which, F is the harmonic transverse dynamic load. In addition $[K_L]$, $[K_{NL}]$ and $[M]$ respectively, are the stiffness linear matrix, stiffness nonlinear matrix and mass matrix. However, using Newmark method, the dynamic deflection of the laminated beam can be derived. Based on this method, Eq. (53) is can be written as (Hajmohammad *et al.* 2017, Keshtegar *et al.* 2020b)

$$\boldsymbol{K}^{*}(\boldsymbol{d}_{i+1}) = \boldsymbol{Q}_{i+1}, \tag{54}$$

In which subscript $i+1$ denotes the time and

$$K^{*}(d_{i+1}) = K_L + K_{NL}(d_{i+1}) + \alpha_0 M, \tag{55}$$

$$Q^{*}_{i+1} = F_{i+1} + M\left(\alpha_0 d_i + \alpha_2 \dot{d}_i + \alpha_3 \ddot{d}_i\right), \tag{56}$$

In which (Karegar et al. 2021)

$$\alpha_0 = \frac{1}{\chi \Delta t^2}, \quad \alpha_1 = \frac{\gamma}{\chi \Delta t}, \quad \alpha_2 = \frac{1}{\chi \Delta t},$$
$$\alpha_3 = \frac{1}{2\chi} - 1, \quad \alpha_4 = \frac{\gamma}{\chi} - 1,$$
$$\alpha_5 = \frac{\Delta t}{2}\left(\frac{\gamma}{\chi} - 2\right), \quad , \alpha_6 = \Delta t\left(1 - \gamma\right), \tag{57}$$
$$\alpha_7 = \Delta t \gamma,$$

In which γ = 0.5 and x=0.25. In addition, the velocity and acceleration vectors are

$$\ddot{d}_{i+1} = \alpha_0(d_{i+1} - d_i) - \alpha_2 \dot{d}_i - \alpha_3 \ddot{d}_i, \tag{58}$$

$$\dot{d}_{i+1} = \dot{d}_i + \alpha_6 \ddot{d}_i + \alpha_7 \ddot{d}_{i+1}, \tag{59}$$

6. Numerical outcomes

In this section, using the DQM, dynamic deflection of the laminated concrete beam is intended and the effect of boundary conditions, volume fraction and agglomeration of nanoparticles, geometrical parameters, porosity parameter on the dynamic displacement of the laminated concrete beam is presented. For this purpose, a laminated porous concrete beam with Young's modulus of E_c = 20 *Gpa* reinforced by nanoparticles with Young's modulus of E_r= 140 *Gpa* is assumed. This section consists of two parts examining the validation and the influences of various parameters on the dynamic displacement of the laminated concrete beam.

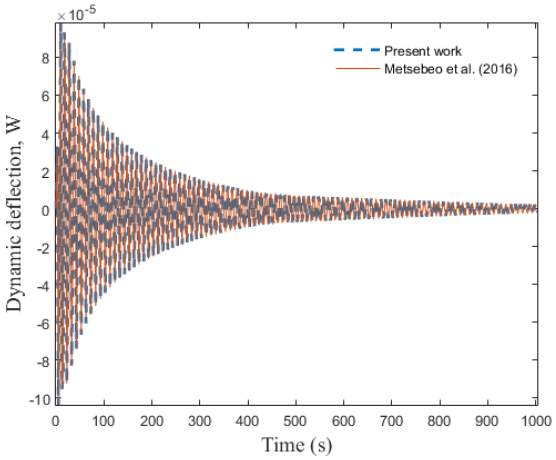

Fig. 2 Validation of this work

6.1 Validation

Dynamic of laminated porous concrete beams reinforced with nanoparticles subjected to harmonic transverse dynamic has not been investigated in the literature. Hence, ignoring the nanoparticles (C_r = 0), damping and porosity, dynamic analysis of a beam subjected to harmonic transverse dynamic with ESST is presented. With the geometric and material parameters the same as Metsebo *et al*. (2016), dynamic deflection was shown in Fig. 2. It is shown that the outcomes of this paper are similar to Metsebo *et al*. (2016) which show that the results are accurate

6.2 Dynamic analysis

The influences of volume percent of nanoparticles on the non-dimensional dynamic deflection of the structure is shown in Fig. 3. It is found that with increasing the nanoparticle volume fraction, the dynamic displacement decreases about 63%. The increase in the volume percent of nanoparticles leads to a reduction in dynamic deflection primarily due to the enhanced stiffness and reinforcing capabilities of the nanoparticles within the composite material. As the volume fraction of nanoparticles rises, their small size allows for efficient integration into the material matrix, reinforcing intermolecular bonds and improving overall structural stiffness. This heightened stiffness effectively resists deformation under dynamic loading conditions, resulting in a decreased dynamic deflection.

The agglomeration of nanoparticles effect on the dynamic displacement of the laminated porous concrete beam is presented in Fig. 4. It is shown that with considering agglomeration, the dynamic deflection is increased about 24%. Agglomeration alters the uniform distribution of nanoparticles, creating regions of concentrated mass or stiffness variations in the material matrix. This non-uniform distribution can lead to local

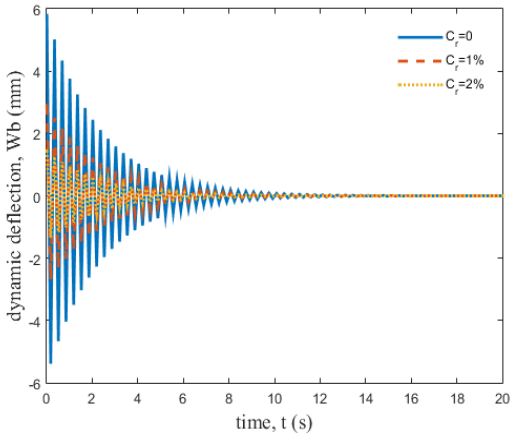

Fig. 3 The influences of nanoparticles on the dynamic displacement of the laminated porous concrete beam

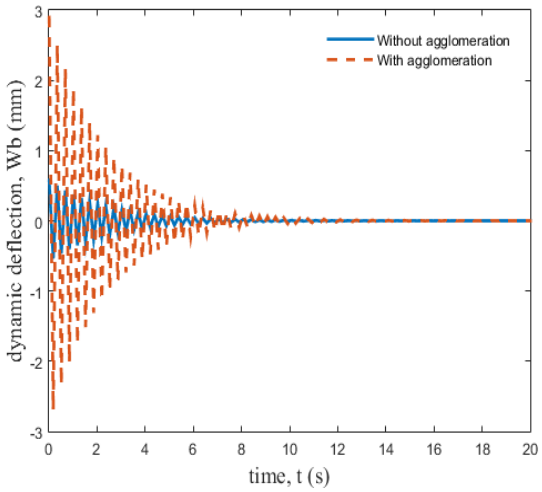

Fig. 4 The influences of agglomeration of nanoparticles on the dynamic displacement of the laminated porous concrete beam

stress concentrations and reduced effectiveness of the reinforcing properties of nanoparticles. In turn, these uneven stress distributions may result in higher susceptibility to dynamic deformation and reduced overall structural stiffness. The agglomerated nanoparticles can act as stress concentrators, promoting localized yielding and deformation, thus contributing to an increased dynamic deflection compared to a scenario with a well-dispersed and uniform distribution of nanoparticles.

The boundary condition influence on the dynamic displacement of the laminated porous concrete beam is presented in Fig. 5. It is found that in the concrete beam with CC boundary condition, the dynamic displacement is reduced about 64%. In a concrete beam with clamped-clamped (CC) boundary conditions, the dynamic displacement is diminished compared to simply supported (SS) and clamped-supported (CS) configurations due to the heightened structural constraints and increased stiffness imposed by the clamped ends. The CC configuration restricts the freedom of dynamic deformation, resulting in a more rigid response.

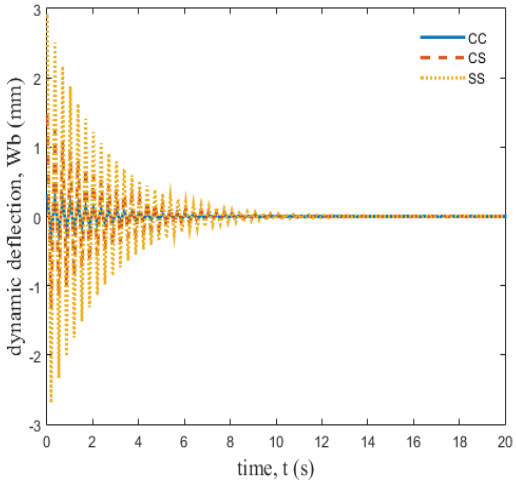

Fig. 5 The influences of boundary condition on the dynamic displacement of the laminated porous concrete beam

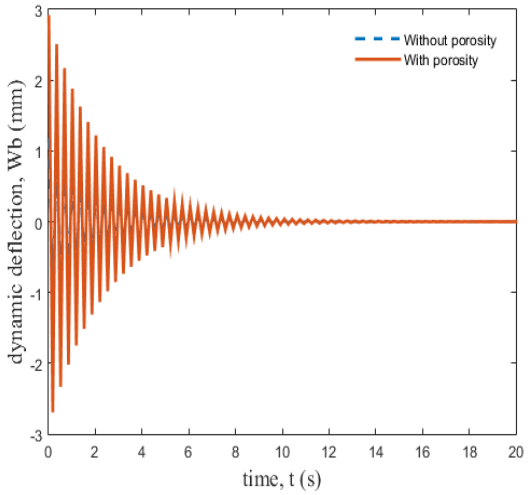

Fig. 6 The influence of porosity on the dynamic displacement of the laminated porous concrete beam

The influences of porosity on the dimensionless dynamic displacement of the laminated porous concrete beam is illustrated in Fig. 6. It can be seen that with considering the porosity, the dynamic displacement increases about 2.8 time. This is reasonable since the incorporation of porosity in a material typically results in an increase in dynamic displacement due to its impact on the material's density, stiffness, and overall mechanical behavior. Porous structures introduce void spaces within the material, reducing its density and, consequently, its stiffness. The lower stiffness of porous materials allows for greater deformation under dynamic loading conditions.

The influence of lamina number on the dynamic displacement of the laminated porous concrete beam is presented in Fig. 7. It is shown enhancing the lamina number up to 5 layers, the dynamic deflection is increased. In addition, with increasing the layer number higher than 5, the dynamic deflection is again increased which shows the best layer number for this structure is 5.

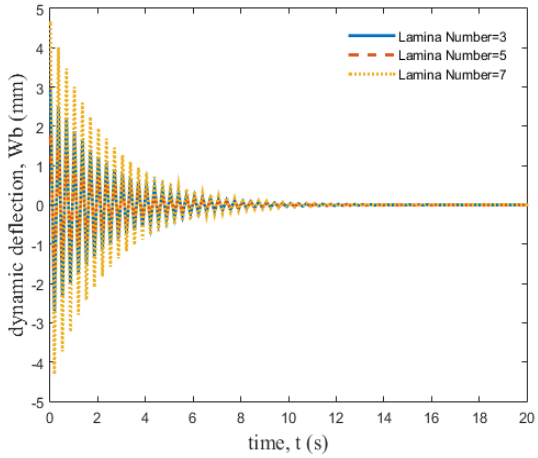

Fig. 7 The influence of lamina number on the dynamic displacement of the laminated porous concrete beam

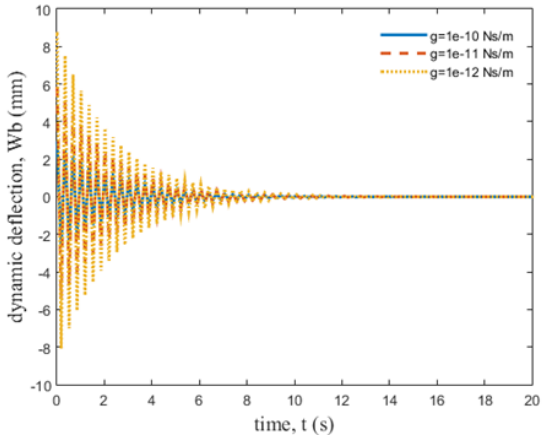

Fig. 8 The influence of structural damping on the dynamic displacement of the laminated porous concrete beam

The influence of structural damping on the dynamic displacement of the laminated porous concrete beam is presented in Fig. 8. It is shown with considering the structural damping, the dynamic deflection decreases. The incorporation of structural damping in a system often leads to a decrease in dynamic deflection due to its dissipative nature. Structural damping involves the conversion of vibrational energy into heat within the material, mitigating the extent of dynamic motion. As the damping ratio increases, the ability of the material to absorb and dissipate vibrational energy improves, resulting in reduced oscillations and dynamic deflection.

7. Conclusions

In-depth research on the use of nanoparticles reinforced composite materials, especially in the field of civil engineering, has attracted increasing interest in recent years but there was very little numerical research to analyze their behavior. In this study, dynamic response of laminated porous concrete beams reinforced with nanoparticles under the harmonic transverse dynamic was studied considering structural damping. The mathematical modeling and theoretical formulation were presented based on ESST and energy method. Using the strain-displacement equations and Hamilton's principle, the final motion equations were obtained. Finally, with Newmark and DQM methods, the dynamic displacement was calculated. The influences of boundary condition, geometrical parameters of beam, volume fraction and agglomeration of nanoparticles, harmonic transverse dynamic load and porosity parameter on the dynamic displacement were presented. Based on the results in this study, the following conclusions can be drawn:

- The presented numerical model was able to capture the behaviour of the porous laminated concrete beam accurately.
- The agglomeration of nanoparticles in the concrete structures can be considered by Mori-Tanaka model.
- With enhancing the nanoparticle volume fraction, the dynamic displacement decreases about 63%.
- The concrete laminated porous beam containing 2% nanoparticles in turns of steel bars exhibited the best performance in terms of decreasing the dynamic deflection.
- It was shown that with assuming agglomeration, the dynamic displacement was increased about 24%.
- It can be seen that with assuming the porosity, the dynamic displacement increases about 2.8 time.
- It was shown with assuming the structural damping, the dynamic displacement reduces.
- The concrete laminated porous beam with 5 layers demonstrated the best performance in terms of decreasing the dynamic deflection.

Findings obtained from this study contain important results for both researchers and practitioners. The most important and interesting of these is that nanoparticles with agglomeration placed in the bending areas of reinforced concrete beams cause a significant decrease in the beam bending capacity, while it increases the capacity up to 2.8 times when used nanoparticles without agglomeration. In fact, it was observed that the amount of layer number of laminated beam at a certain value of 5 has a positive effect on the stiffness. This result derived from the study is an important finding especially for designers. In addition, the stiffness of the concrete beam strengthened by nanoparticles are suitable for decreasing the dynamic deflection of structures and improve the tensile strength of the concrete.

References

Aksoylu, C., Yazman, Ş., Özkılıç, Y.O., Gemi, L. and Arslan, M.H. (2020b), "Experimental analysis of reinforced concrete shear deficient beams with circular web openings strengthened by CFRP composite", *Compos. Struct.*, **249**, 112561. https://doi.org/10.1016/j.compstruct.2020.112561.

Aksoylu, C., Özkılıç, Y.O. and Arslan, M.H. (2020a), "Damages on prefabricated concrete dapped-end purlins due to snow loads and a novel reinforcement detail", *Eng. Struct.*, **225**, 111225. https://doi.org/10.1016/j.engstruct.2020.111225.

Aksoylu, C., Özkılıç, Y.O., Yazman, Ş., Gemi, L. and Arslan, M.H. (2021), "İnceltilmiş Uçlu Önüretimli Aşık Kirişlerinin Yük Taşıma Kapasitelerinin Deneysel ve Numerik Olarak İrdelenmesi ve Çözüm Önerileri", *Teknik Dergi.*, **32**(3), 10823-10858. https://doi.org/10.18400/tekderg.667066. (In Turkish).

Al-Furjan, M.S.H., Farrokhian, A., Mahmoud, S.R. and Kolahchi, R. (2021), "Dynamic deflection and contact force histories of graphene platelets reinforced conical shell integrated with magnetostrictive layers subjected to low-velocity impact", *Thin. Wall. Struct.*, **163**, 107706.https://doi.org/10.1016/j.tws.2021.107706.

Alijani, M. and Rabani Bidgoli, M. (2018), "Agglomerated SiO_2 nanoparticles reinforced-concrete foundations based on higher order shear deformation theory: Vibration analysis", *Adv. Concr. Constr.*, **6**(6), 585-610. http://dx.doi.org/10.12989/acc.2018.6.6.585.

Alipour, M.M. and Shariyat, M. (2019), "Nonlocal zigzag analytical solution for Laplacian hygrothermal stress analysis of annular sandwich macro/nanoplates with poor adhesions and 2D-FGM porous cores", *Arch. Civ. Mech. Eng.*, **19**(4), 1211-1234. https://doi.org/10.1016/j.acme.2019.06.008.

Amoli, A., Kolahchi, R. and Rabani Bidgoli, M. (2018), "Seismic analysis of AL2O3 nanoparticles-reinforced concrete plates based on sinusoidal shear deformation theory", *Earthq. Struct.*, **15**(3), 285-294. https://doi.org/10.12989/eas.2018.15.3.285.

Anirudh, B., Ben Zineb, T., Polit, O., Ganapathi, M. and Prateek, G. (2020), "Nonlinear bending of porous curved beams reinforced by functionally graded nanocomposite grapheme platelets applying an efficient shear flexible finite element approach", *Int. J. Nonlinear. Mech.*, **119**, 103346. https://doi.org/10.1016/j.ijnonlinmec.2019.103346.

Azree, M. and Wang, Y.C. (2012), "Mechanical properties of foamed concrete exposed to high temperatures", *Constr. Build. Mater.*, **26**(1), 638-654. https://doi.org/10.1016/j.conbuildmat.2011.06.067.

Bai, Z., Liu, Y., Yang, J. and He, S. (2019), "Exploring the dynamic response and energy dissipation capacity of functionally graded EPS concrete", *Constr. Build. Mater.*, **227**, 116574. https://doi.org/10.1016/j.conbuildmat.2019.07.300.

Bakhshande, Amnieh. H., Zamzam, M.S. and Kolahchi, R. (2018), "Dynamic analysis of non-homogeneous concrete blocks mixed by SiO_2 nanoparticles subjected to blast load experimentally and theoretically", *Constr. Build. Mater.*, **174**, 633-644. https://doi.org/10.1016/j.conbuildmat.2018.04.140.

Bedia, W.A., Houari, M.S.A., Bessaim, A., Bousahla, A.A., Tounsi, A., Saeed, T. and Alhodaly, M.S. (2019), "A new hyperbolic two-unknown beam model for bending and buckling analysis of a nonlocal strain gradient nanobeams", *J. Nano Res.*, **57**, 175-191, https://doi.org/10.4028/www.scientific.net/JNanoR.57.175.

Bendaida, M., Bousahla, A.A., Mouffoki, A., Heireche, H., Bourada, F., Tounsi, A., Benachour, A., Tounsi, A. and Hussain, M. (2021), "Dynamic properties of nonlocal temperature-dependent FG nanobeams under various thermal environments", *Trans. Porous Media*, **142**, 187-208. https://doi.org/10.1007/s11242-021-01666-3.

Chan, R., Liu, X. and Galobardes, I. (2020), "Parametric study of functionally graded concretes incorporating steel fibres and recycled aggregates", *Constr. Build. Mater.*, **242**, 118186. https://doi.org/10.1016/j.conbuildmat.2020.118186.

Craveiro, F., Nazarian, S., Bartolo, H., Bartolo, H., Bartolo, P.J. and Duarte, J.P. (2020), "An automated system for 3D printing functionally graded concrete-based materials", *Addit. Manuf.*, **33**, 101146. https://doi.org/10.1016/j.addma.2020.101146.

Draiche, K., Bousahla, A.A., Tounsi, A. and Hussain, M. (2021), "An integral shear and normal deformation theory for bending analysis of functionally graded sandwich curved beams", *Arch. Appl. Mech.*, **91**, 4669-4691. https://doi.org/10.1007/s00419-021-02005-0.

Fouaidi, M., Jamal, M. and Belouaggadia, N. (2020), "Nonlinear bending analysis of functionally graded porous beams using the multiquadric radial basis functions and a Taylor series-based continuation procedure", *Compos. Struct.*, **252**, 112593. https://doi.org/10.1016/j.compstruct.2020.112593.

Fouaidi, M., Jamal, M., Zaite, A. and Belouaggadia, N. (2021), "Bending analysis of functionally graded graphene oxide powder-reinforced composite beams using a meshfree method", *Aerosp. Sci. Technol.*, **110**, 106479. https://doi.org/10.1016/j.ast.2020.106479.

Gemi, L., Aksoylu, C., Yazman, Ş., Özkılıç, Y.O. and Arslan M.H. (2019), "Experimental investigation of shear capacity and damage analysis of thinned end prefabricated concrete purlins strengthened by CFRP composite", *Compos. Struct.*, **229**, 111399. https://doi.org/10.1016/j.compstruct.2019.111399.

Hajmohammad, M.H., Sharif Zarei, M., Nouri, A. and Kolahchi, R. (2017), "Dynamic buckling of sensor/functionally graded-carbon nanotube-reinforced laminated plates/actuator based on sinusoidal-visco-piezoelasticity theories", *J. Sandw. Struct. Mater.*, https://doi.org/10.1177/1099636217720373.

Harith, I.K. (2018), "Study on polyurethane foamed concrete for use in structural applications", *Case Stud. Constr. Mater.*, **8**, 79-86. https://doi.org/10.1016/j.cscm.2017.11.005.

Heidarzadeh, A., Kolahchi, R. and Rabani Bidgoli, M. (2018), "Concrete pipes reinforced with AL2O3 nanoparticles considering Agglomeration: Magneto-Thermo-Mechanical Stress Analysis", *Int. J. Civ. Eng.*, **16**(3), 315-322. https://doi.org/10.1007/s40999-016-0130-2.

Jafarian Arani, A. and Kolahchi, R. (2016), "Buckling analysis of embedded laminated porous concrete beams armed with carbon nanotubes", *Comput. Concret.* **17**, 567-578.

Jassas, M.R., Rabani Bidgoli, M. and Kolahchi, R. (2019), "Forced vibration analysis of concrete slabs reinforced by agglomerated SiO_2 nanoparticles based on numerical methods", *Constr. Build. Mater.*, **211**, 796-806. https://doi.org/10.1016/j.conbuildmat.2019.03.263.

Karegar, M., Rabani Bidgoli, M. and Mazaheri, H. (2021), "Smart control and seismic analysis of concrete frames with piezoelectric layer based on mathematical modelling and numerical method", *Structures*, **32**, 1171-1179.

Kargar, M. and Rabani Bidgoli, M. (2018), "Mathematical modeling of smart nanoparticles-reinforced concrete foundations: Vibration analysis", *Geomech. Eng.*, **27**(4), 465-477. https://doi.org/10.12989/gae.2018.27.4.465.

Keshtegar, B., Motezaker, M., Kolahchi, R. and Trung, N.T. (2020a), "Wave propagation and vibration responses in porous smart nanocomposite sandwich beam resting on Kerr foundation considering structural damping", *Thin Wall. Struct.*, **154**, 106820.

Keshtegar, B., Farrokhian, A., Kolahchi, R. and Trung, N.T. (2020b), "Dynamic stability response of truncated nanocomposite conical shell with magnetostrictive face sheets utilizing higher order theory of sandwich panels", *Eur. J. Mech. A Solids.*, **82**, 104010.

Madenci, E., Özkılıç, Y.O. and Gemi, L. (2020a), "Theoretical investigation on static analysis of pultruded GFRP composite beams", *J. Eng. Sci.*, **8**(3), 483-490. https://doi.org/10.21541/apjes.734770.

Madenci, E., Özkılıç, Y.O. and Gemi, L. (2020b), "Buckling and free vibration analyses of pultruded GFRP laminated composites: Experimental, numerical and analytical investigations", *Compos. Struct.*, **254**, 112806. https://doi.org/10.1016/j.compstruct.2020.112806.

Madenci, E., Özkılıç, Y.O. and Gemi, L. (2020c), "Experimental and theoretical investigation on flexure performance of

pultruded GFRP composite beams with damage analyses", *Compos. Struct*., **242**, 112162. https://doi.org/10.1016/j.compstruct.2020.112162.

Madenci, E. and Özkılıç, Y.O. (2021), "Free vibration analysis of open-cell FG porous beams: analytical, numerical and ANN approaches", *Geomech. Eng*., **40**(2), 157-173. https://doi.org/10.12989/gae.2021.40.2.157.

Mahjoobi, M. and Rabani Bidgoli, M. (2019), "Vibration analysis of concrete foundation armed by silica nanoparticles based on numerical methods", *Struct. Eng. Mech*., **69**(5), 547-555. http://dx.doi.org/10.12989/sem.2019.69.5.547**.**

Metsebo, J., Nana Nbendjo, B.R. and Woafo, P. (2016), "Dynamic responses of a hinged-hinged Timoshenko beam with or without a damage subject to blast loading", *Mech. Res. Commun*., **71**, 38-43.

Mesbah, A., Belabed, Z., Amara, K., Tounsi, A., Bousahla, A.A. and Bourada, F. (2023), "Formulation and evaluation a finite element model for free vibration and buckling behaviours of functionally graded porous (FGP) beams", *Struct. Eng. Mech.*, **86**, 291-309, https://doi.org/10.12989/sem.2023.86.3.291.

Motezaker, M., Kolahchi, R., Kumar Rajak, D. and Mahmoud, S. R. (2021), "Influences of fiber reinforced polymer layer on the dynamic deflection of concrete pipes containing nanoparticle subjected to earthquake load", *Polym. Compos*., https://doi.org/10.1002/pc.26118.

Mouaici, F., Bouadi, A., Bendaida, M., Draiche, K., Bousahla, A.A., Bourada, F., Tounsi, A., Ghazwani, M.H. and Alnujaie, A. (2022), "Investigation of the mechanical behavior of functionally graded sandwich thick beams", *Steel Compos. Struct.,* **44**(5), 707-726, https://doi.org/10.12989/scs.2022.44.5.707.

Özkılıç, Y.O., Aksoylu, C. and Arslan M.H. (2021a), "Numerical evaluation of effects of shear span, stirrup spacing and angle of stirrup on reinforced concrete beam behaviour", *Struct. Eng. Mech*., **79**(3), 309-326. https://doi.org/10.12989/sem.2021.79.3.309.

Özkılıç, Y.O., Aksoylu, C. and Arslan M.H. (2021b), "Experimental and numerical investigations of steel fiber reinforced concrete dapped-end purlins", *J. Build. Eng*., **36**, 102119. https://doi.org/10.1016/j.jobe.2020.102119.

Özkılıç, Y.O., Yazman, Ş., Aksoylu, C., Arslan M.H. and Gemi, L. (2021c), "Numerical investigation of the parameters influencing the behavior of dapped end prefabricated concrete purlins with and without CFRP strengthening", *Constr. Build. Mater*., **275**, 122173. https://doi.org/10.1016/j.conbuildmat.2020.122173.

Penna, R., Feo, L. and Lovisi, G. (2021), "Hygro-thermal bending behavior of porous FG nano-beams via local/nonlocal strain and stress gradient theories of elasticity", *Compos. Struct*., **263**, 113627. https://doi.org/10.1016/j.compstruct.2021.113627.

Pietras, D. and Sadowski, T. (2019), "A numerical model for description of mechanical behaviour of a Functionally Graded Autoclaved Aerated Concrete created on the basis of experimental results for homogenous Autoclaved Aerated Concretes with different porosities", *Constr. Build. Mater*., **204**, 839-848. https://doi.org/10.1016/j.conbuildmat.2019.01.189.

Polit, O., Anant, C., Anirudh, B. and Ganapathi, M. (2019), "Functionally graded graphene reinforced porous nanocomposite curved beams: Bending and elastic stability using a higher-order model with thickness stretch effect", *Compos. B Eng*., **166**, 310-327. https://doi.org/10.1016/j.compositesb.2018.11.074.

Reed, N. (2002), *Mechanics of Laminated Composite Plates and Shells*, CRC Press, 2003.

Sahoo, S.K., Mohapatra, B.G., Patro, S.K. and Acharya, P.K. (2021), "Evaluation of graded layer in ground granulated blast furnace slag based layered concrete", *Constr. Build. Mater*., **276**, 122218. https://doi.org/10.1016/j.conbuildmat.2020.122218.

Sang, G., Zhu, Y., Yang, G. and Zhang, H. (2015), "Preparation and characterization of high porosity cement-based foam material", *Constr. Build. Mater*., **91**, 133-137. https://doi.org/10.1016/j.conbuildmat.2015.05.032.

Shagholani Loor, A., Rabani Bidgoli, M. and Mazaheri, H. (2020), "On the use of differential quadrature-three-term conjugate finite-step length methods for reliability analysis of steel fiber-reinforced sinusoidal rupture beams", *Eng. Comput*., https://doi.org/10.1007/s00366-020-01201-w.

Sridhar, R. and Prasad, D.R. (2019), "Damage assessment of functionally graded reinforced concrete beams using hybrid fiber engineered cementitious composites", *Structures*, **20**, 832-847. https://doi.org/10.1016/j.istruc.2019.07.002.

Taherifar, R., Zareei, S.A., Bidgoli, M.R. and Kolahchi, R. (2020), "Seismic analysis in pad concrete foundation reinforced by nanoparticles covered by smart layer utilizing plate higher order theory", *Geomech. Eng*., **37**(1), 99-115. https://doi.org/10.12989/gae.2020.37.1.099.

Tounsi, A., Bousahla, A.A., Tahir, S.I., Hadj Mostefa, A., Bourada, F., Al-Osta, M.A. and Tounsi, A. (2023), "Influences of different boundary conditions and hygro-thermal environment on the free vibration responses of FGM sandwich plates resting on viscoelastic foundation", *Int. J. Struct. Stab. Dynam*., In press, https://doi.org/10.1142/S0219455424501177.

Viet, N.V. and Zaki, W. (2021), "Bending model for functionally graded porous shape memory alloy/poroelastic composite cantilever beams", *Appl. Math. Model*., **97**, 398-417. https://doi.org/10.1016/j.apm.2021.03.058.

Zamani, A. and Rabani Bidgoli, M. (2017), "Vibration analysis of concrete foundations retrofit with NFRP layer resting on soil medium using sinusoidal shear deformation theory", *Soil Dyn. Earthq. Eng*., **103**, 141-150. https://doi.org/10.1016/j.soildyn.2017.09.018.

Zamanian, M., Kolahchi, R. and Rabani Bidgoli, M. (2017), "Agglomeration effects on the buckling behaviour of embedded concrete columns reinforced with SiO_2 nanoparticles", *Wind Struct*., **24**(1), 43-57. https://doi.org/10.12989/was.2017.24.1.043.

Zhang, W., Qin, Q., Li, K., Li, J. and Wang, Q. (2021), "Effect of stepwise gradient on dynamic failure of composite sandwich beams with metal foam core subject to low-velocity impact", *Int. J. Solids. Struct*., **228**, 111125. https://doi.org/10.1016/j.ijsolstr.2021.111125.

CC